

A PROPOSAL TO MEASURE
SINGLE AND DOUBLE DIFFRACTION DISSOCIATION
AT THE FERMILAB $\bar{p}p$ COLLIDER

T.J. Chapin, R.L. Cool, K. Goulianos, K.A. Jenkins,
H. Sticker and S.N. White

The Rockefeller University
New York, N.Y. 10021

September 1, 1982

SPOKESMAN: K. Goulianos

Telephone: 212/570-8827

A PROPOSAL TO MEASURE
SINGLE AND DOUBLE DIFFRACTION DISSOCIATION
AT THE FERMILAB $\bar{p}p$ COLLIDER

SUMMARY

We propose to measure the inclusive differential cross sections $d\sigma/dM^2$ and $d^2\sigma/dM_1^2 dM_2^2$ for the single and double diffraction dissociation processes $\bar{p}p \rightarrow Xp$ and $pp \rightarrow X_1 + X_2$, and the charged multiplicity distributions of the diffractive states X at the Fermilab $\bar{p}p$ Collider. The differential cross sections will be normalized to the total inelastic $\bar{p}p$ cross section.

The experimental method consists in measuring the polar angle of all charged particles of an event using scintillation counter hodoscopes. The recoil particle, p or \bar{p} , is not detected. The diffractive mass is calculated from the mean angle of the charged secondaries. The charged multiplicity distribution as a function of mass is obtained from the total event sample.

The apparatus is made of 5cm wide by 10 to 60cm long scintillation counters, covering the entire solid angle outside the beam pipes. Elastic events are not detected. A total of 420 counters are employed.

At a luminosity of $10^{28} \text{ cm}^{-2} \text{ sec}^{-1}$, a total of $\sim 2 \times 10^5$ events/hr will be registered, approximately one half of which will be diffractive. Within the full width of the M_x^2 resolution, $\sim 10^4$ /hr single diffraction and ~ 400 /hr double diffraction dissociation events are expected in the region $1-x = 0.1$. Thus, 500 hours of running will be sufficient for the proposed study even if the luminosity is down by two orders of magnitude, as may be the case in the initial stages of the operation of the Collider.

TABLE OF CONTENTS

I. INTRODUCTION	1
II. MOTIVATION	1
III. EXPERIMENTAL METHOD	5
IV. APPARATUS	12
V. EVENT RATES AND RUNNING TIME	13
VI. LOCATION OF EXPERIMENT	15
REFERENCES	16
FIGURE CAPTIONS	17
FIGURES	19

A PROPOSAL TO MEASURE
SINGLE AND DOUBLE DIFFRACTION DISSOCIATION
AT THE FERMILAB $\bar{p}p$ COLLIDER

I. INTRODUCTION

We propose an experimental study of the inclusive single and double diffraction dissociation processes

$$\bar{p}p \rightarrow Xp ; \quad \bar{p}p \rightarrow \bar{p}X \quad (1)$$

$$\bar{p}p \rightarrow X_1 + X_2 \quad (2)$$

at the Fermilab $\bar{p}p$ collider ($\sqrt{s}=2000$ GeV). Specifically, we will measure:

- (i) The differential cross sections $d\sigma/dM_X^2$ and $d^2\sigma/dM_1^2 dM_2^2$ for processes (1) and (2).
- (ii) The charged multiplicity distribution of the diffractive state at each mass M_X .

The diffractive cross sections will be normalized to the total inelastic $\bar{p}p$ cross section. The t -values will not be measured. The differential cross sections will, therefore, represent integrals over t and will be functions only of M_X^2 , as indicated in (i) above.

II. MOTIVATION

The inclusive single diffraction dissociation of hadrons

$$h + p \rightarrow X + p \quad (h=p^\pm, K^\pm, \pi^\pm) \quad (3)$$

has been studied at Fermilab and at the ISR. Precise measurements of the differential cross sections

$$d^2\sigma^h/dtdM_X^2 = f_h(s, t, M_X^2) \quad (4)$$

have unveiled a simple and universal behavior which is summarized below^[1]:

- (i) Small s -dependence, leading asymptotically to differential cross sections independent of s .
- (ii) Exponential behavior in t , $d\sigma/dt \sim \exp(b_D t)$, with a slope parameter, b_D , approximately equal to one half that of the corresponding elastic scattering process.
- (iii) Mass spectra varying as $1/M_x^2$.
- (iv) Factorization of the diffractive vertex, as evidenced by the scaling of the diffractive cross sections to the corresponding total cross sections.

This behavior can be explained by triple-Pomeron dominance in the diffractive amplitude and is therefore expected by the modern, more complete Regge-type theory, the Critical Pomeron Reggeon Field Theory^[2]. The theory also predicts the rise of total cross sections with energy, attributing it mostly to diffraction.

The question as to how much of the rise of the pp inelastic cross section comes from diffraction dissociation is answered experimentally^[1] in Figure 1. The dotted band represents the inelastic cross section after subtracting twice the value of the single diffraction dissociation cross section given by

$$\sigma_{SD} (pp \rightarrow Xp) = (0.68 \pm 0.05) \left(1 + \frac{36 \pm 8}{s}\right) \ln(0.1s) \quad (5)$$

The increase of $\sigma_{in} - 2\sigma_{SD}$ with energy is small, indicating that the bulk of the rise of σ_{in} is due to single diffraction dissociation. The remaining rise is probably due to double diffraction dissociation. The inclusive double diffraction dissociation cross section, σ_{DD} , has not been measured at Fermilab or at the ISR. The measurement is difficult since the momenta of all secondary particles, including neutrals, are required for determining the diffractive masses (our method avoids this problem -- see Section III). Using factorization, one obtains

$$\sigma_{DD} = \frac{b_{SD}^2}{b_{el}(2b_{SD} - b_{el})} \frac{\sigma_{SD}^2}{\sigma_{el}} = K_{DD} \frac{\sigma_{SD}^2}{\sigma_{el}} \quad (6)$$

where b_{SD} and b_{el} are the slope parameters of single diffraction dissociation and of elastic scattering, respectively. Since $b_{SD} \sim (1/2) b_{el}$, the numerical value of the coefficient K_{DD} is very sensitive to the ratio b_{SD}/b_{el} . As an order of magnitude estimate, taking this ratio to be 2/3 yields $K_{DD} = 1.33$, resulting in $\sigma_{DD} = 2.8$ mb at 2000 GeV/c, which is sufficient to explain the rise in $\sigma_{in} - 2\sigma_{SD}$. Thus, the total inelastic cross section, which may be written as

$$\sigma_{in} = \sigma_0 + 2\sigma_{SD} + \sigma_{DD} \quad (7)$$

appears to have a hard core, σ_0 , that remains constant over the entire energy region from just above threshold to the highest ISR energy. The value of σ_0 is 26.3 mb.

In this experiment, we will measure $d\sigma/dM^2$ and $d^2\sigma/dM_1^2 dM_2^2$ for single and double diffraction dissociation, respectively, normalized to σ_{in} . The $1/M^2$ behavior will be checked to masses as high as $M^2 \approx 0.1s$ ($M=632$ GeV for $\sqrt{s}=2000$ GeV). The diffractive cross sections will then be integrated over M^2 , yielding σ_{SD}/σ_{in} and σ_{DD}/σ_{in} . The ratio σ_0/σ_{in} will also be obtained experimentally.

If the mass spectrum turns out to vary as $1/M_x^2$, it will be reasonable to assume that the single diffraction dissociation cross section at these energies is given correctly by Eq. (5) and, therefore, the diffractive events

may be used to yield the absolute normalization. The cross sections σ_{in} and σ_0 may then be obtained, and σ_0 may be compared to 26.3 mb to check whether the magnitude of the hard core has increased. Although present theories do not expect σ_0 to remain constant as the energy increases, an experimental measurement of the energy dependence of the hard core is of great interest to all theories. The value of σ_{in} may also be obtained directly by measuring the luminosity, yielding an assumption-free absolute normalization for σ_{SD} , σ_{DD} and σ_0 .

The charged multiplicity distributions of the diffractive states of hadrons are strikingly simple and universal^[3]. They are described well by a Gaussian function that depends only on the available mass for pion production, $M = M_x - M_h$, peaks at $n_0 = 2M^{\frac{1}{2}}$, where M is in GeV, and has a peak to width ratio $n_0/D = 2$, where $D = (\overline{n^2} - n_0^2)^{\frac{1}{2}}$. This function seems to hold for the hard core as well, providing a universal description of all hadronic multiplicities^[4]. In this experiment, the range of diffractive masses will be extended by a factor of 35, from 18 GeV (ISR) to 630 GeV. It will be interesting to see whether the above description still holds. In any case, it will be interesting to compare the mass dependence of the diffractive multiplicities with the \sqrt{s} dependence of the multiplicity of the hard core. We believe that treating diffractive and non-diffractive multiplicities separately is essential to the understanding of the process of hadronization.

III. EXPERIMENTAL METHOD

At Fermilab and at the ISR, inclusive single diffraction dissociation was measured by the recoil technique. The diffractive mass was calculated from the forward component of the momentum of the recoiling proton:

$$M_x^2/s \cong 1-x = 1 - 2 p_{||}^* / \sqrt{s} \quad (8)$$

A mass resolution of $\delta M/M$ requires an accuracy in the momentum measurement of

$$\frac{\delta p_{||}^*}{p_{||}^*} = 2(1-x) \frac{\delta M}{M} \quad (9)$$

For $\delta M/M = 10\%$ at the typical value of $1-x = 0.05$, $\delta p_{||}^* / p_{||}^* = 1\%$. At the Fermilab collider, recoils of interest have $p_{||} \cong 1000$ GeV/c and $\langle p_{\perp} \rangle \cong 0.3$ GeV/c ($d\sigma/dt \sim e^{8t}$), hence an average polar angle of about 0.3 mrad. A 1% measurement of the momentum of such a particle is a formidable task. Below, we describe a method of determining M_x to the accuracy of $\sim 10\%$ using the dissociation products.

The method consists in measuring the polar angle of all the charged particles associated with the decay of the mass M_x . For a decay which is isotropic in the center of mass of the state X , the angular distribution is given by

$$\frac{dn_c}{d \cos \theta} = n_c \frac{1 - \beta_x^2}{2(1 - \beta_x \cos \theta)^2} \quad (10)$$

where n_c is the total number of charged particles in the decay and β_x is the velocity of the mass M_x . The mean angle, $\bar{\theta}$, defined as the angle dividing n_c into two halves, is related to the diffractive mass by

$$\cos \bar{\theta} = \beta_x = \frac{1 - M_x^2/s}{1 + M_x^2/s} \quad (11)$$

This relationship holds even in the case of a non-isotropic decay distribution, provided the distribution is fore-aft symmetric. For $M^2/s = 0.1$, $\bar{\theta} = 35^\circ$. For $M = 18$ GeV, the mass value for which $M^2/s = 0.1$ at the ISR, the mean angle at the Fermilab collider is 18 mrad, corresponding to a distance 18cm away from the beam 10m downstream of the interaction region. Thus, the study of diffraction dissociation into masses higher than those observed at the ISR involves secondary particles at angles that are large enough to be measured with scintillation counter hodoscopes located outside the beam pipe. Inverting Eq. (11) yields

$$\frac{M_x^2}{s} = \frac{1 - \cos \bar{\theta}}{1 + \cos \bar{\theta}} \quad (12)$$

which, for $M_x^2/s < 0.1$, can be approximated by

$$M_x = \frac{\sqrt{s}}{2} \bar{\theta} \quad (13)$$

For $\sqrt{s} = 2000$ GeV, $M_x(\text{GeV}) \approx \bar{\theta}$ (mrad); i.e., the diffractive mass (in GeV) at the Fermilab collider is equal to the mean angle (in mrad) of the dissociation products.

The accuracy to which M_x can be determined by this method is limited by the fluctuations in $\bar{\theta}$ caused by the finite number of charged particles in the final state. The average number of charged particles expected from the decay of a diffractive mass M_x is

$$\bar{n}_c = 2 M_x^{\frac{1}{2}} \quad (M_x \text{ in GeV}) \quad (14)$$

The uncertainty in M_x is best calculated by rewriting Eqs. (10) and (11) in terms of the pseudo-rapidity variable η , which is related to the polar angle by

$$\eta = -\ln \tan \frac{\theta}{2} \quad (15)$$

In the mass region of interest, the pseudo-rapidity η is approximately equal to the rapidity y , hence the two terms will be used interchangeably.

The rapidity distribution of the charged particles from an isotropic decay of the mass M_x is

$$\frac{dn_c}{d\eta} = \frac{2n_c}{(e^{\eta'} + e^{-\eta'})^2} \quad ; \quad \eta' = \eta - \bar{\eta} \quad (16)$$

where $\bar{\eta}$, the average rapidity of the particles, which is equal to the rapidity of the mass M_x , is given by

$$\bar{\eta} = \eta_M = \frac{1}{2} \ln \frac{s}{M_x^2} \quad (17)$$

The distribution represented by Eq. (16) is plotted in Figures 2 and 3. It is very similar to a Gaussian function with a standard deviation

$$\Delta\eta' \cong \pm 0.7 \quad (18)$$

The uncertainty in determining $\bar{\eta}$ for a cluster consisting of n_c charged particles is given by

$$\Delta\bar{\eta} = \frac{\Delta\eta'}{\sqrt{\bar{n}_c}} \quad (19)$$

From Eq. (17), $\Delta M_x/M_x = \Delta\bar{\eta}$. Thus, the mass resolution is

$$\frac{\Delta M_x}{M_x} = \pm \frac{0.7}{\sqrt{2M_x^{\frac{1}{2}}}} = \pm \frac{0.5}{M_x^{\frac{1}{2}}} = \pm \frac{0.5}{[(1-x)s]^{1/8}} \quad (20)$$

where we have used $\bar{n}_c = 2M_x^{\frac{1}{2}}$ (Eq. 14) in place of n_c in Eq. (19) and hence this result represents the mass resolution at the average charged multiplicity of the diffractive state. For non-isotropic decays, the clusters will be wider in rapidity and the mass resolution correspondingly larger. However, as mentioned earlier, M_x will still be obtained correctly from $\bar{\eta}$ using Eq. (17).

Results^[5] from the Pisa-Stony Brook experiment at the ISR (Figs. 4 and 5) are consistent with Eqs. (16) and (18) and, therefore, with isotropy in diffraction dissociation. Figure 4 shows the $\bar{\eta}$ distribution of events with a given multiplicity for various values of $\Delta\eta'$ (called $\Delta\eta$ in the figure). For diffractive events, a given multiplicity corresponds, on the average, to a given mass (see Eq. 14). In Figure 4, events with $\Delta\eta$ in the range 0.6 to 1.0 show two distinct peaks at two values of $\bar{\eta}$ which are symmetric around $\bar{\eta} = 0$. These peaks are presumably due to diffraction dissociation of the two beam protons. Thus, the diffractive clusters do indeed have a width compatible with ± 0.7 as required by isotropy. The $\bar{\eta}$ width of these peaks (not to be confused with $\Delta\eta$) is due to the fact that a given charged multiplicity comes from a range of diffractive masses around the "average" mass. As $\Delta\eta$ increases, the diffractive peaks disappear while a central peak, presumably due to "hard core" collisions, appears around $\bar{\eta} = 0$. This is shown better in Figure 5 which represents three-dimensional plots of "events versus $\bar{\eta}$ and $\Delta\eta$ " for various charged

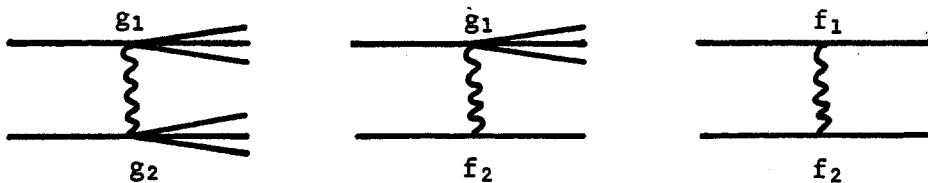
multiplicities (corresponding to various diffractive masses). As the multiplicity increases, the ratio of central to diffractive events increases while, at the same time, the diffractive peaks move closer to $\bar{\eta} = 0$. However, the width $\Delta\eta$ of the diffractive peaks stays constant at $\sim \pm 0.7$ as expected for isotropic decays. Non-diffractive events centered around $\bar{\eta} = 0$ have rapidity widths much larger than ± 0.7 . Therefore, high mass diffractive events, which have $\bar{\eta}$ close to zero, may be separated from non-diffractive ones on the basis of the width of their rapidity distributions.

Figure 6 shows^[6] the inclusive differential cross section $d^2\sigma/dtM_x^2$ as a function of M_x^2 for $pp \rightarrow Xp$ at $s = 500 \text{ GeV}^2$. For $M_x^2 \gtrsim 50 \text{ GeV}^2$ or $1-x \gtrsim 0.1$, the cross section is higher than that expected from the $1/M_x^2$ extrapolation, presumably due to non-diffractive contributions. A recoil experiment at the Fermilab collider would be expected to yield similar results. The broken line in Figure 7 indicates this behavior. If the diffractive events were separated from the non-diffractive ones, one would obtain the solid rather than the broken curve in Figure 7. The ladder-like steps indicate the full width of the mass resolution. The cross section represented by the area between the broken and solid curves on both sides of $1-x = 1$ (assuming that the curves repeat symmetrically on the right side of $1-x = 1$ due to dissociation of the "other" proton) is 26.3 mb; i.e., the "hard core" cross section of Figure 1. The curving of the $1/M_x^2$ line downwards at $1-x \approx 0.35$ represents the cut-off due to t_{\min} , where $|t_{\min}| = [M_p(1-x)]^2$. The cut-off corresponds to $\exp(b_D t_{\min}) = e^{-1}$ with $b_D \approx 10 \text{ (GeV/c)}^{-2}$. Rejection of non-diffractive events will bring down the level of the broken curve and will thus extend the study of diffraction dissociation into the region of $M_x^2/s \gtrsim 0.1$. Figure 8 shows $d\sigma/dM_x^2$ versus M_x^2 . Without identification of the diffractive events, using this technique at the ISR would yield a marginal diffractive peak in the inclusive

mass spectrum, represented in the figure by the broken line. With event-type identification, such as that based on rapidity distribution widths, the diffractive peak would stand out. Depending on the success of the event identification method, the diffractive peak at the Fermilab Collider will be studied over 4 to 6 orders of magnitude, up to masses of 500 to 1000 GeV!!

The inclusive double diffraction dissociation process, $\bar{p} + p \rightarrow X_1 + X_2$, can be studied by fitting events for two clusters, one on each side of the interaction region, using Eqs. (16) and (17). As in single diffraction dissociation, the widths of the rapidity distributions may prove useful in identifying doubly diffractive events. In the fits, the actual rapidity widths measured in single diffraction dissociation will be used, rather than the width of ± 0.7 (eq. 18) which is based on the assumption of isotropy in the decay of the diffractive mass.

The differential cross section $d^2\sigma/dM_1^2 dM_2^2$ will be measured and normalized to the total inelastic cross section. It may also be compared directly to the cross section $d\sigma/dM^2$ of single diffraction dissociation. As discussed previously, double diffraction dissociation is related to single diffraction and to elastic scattering through factorization. The amplitudes for these three processes are drawn below:



Clearly,

$$(g_1 g_2)^2 = \frac{(g_1 f_2)^2 (f_1 g_2)^2}{(f_1 f_2)^2} \quad (21)$$

Factorization states that each amplitude is proportional to the product of the coupling constants at its two vertices. Therefore, Eq. (21) leads to

$$\frac{d^3\sigma}{dt dM_1^2 dM_2^2} = \frac{d^2\sigma}{dt dM_1^2} \cdot \frac{d^2\sigma}{dt dM_2^2} / \left(\frac{d\sigma_{el}}{dt} \right) \quad (22)$$

Assuming the form $\exp(bt)$ both for single diffraction and for elastic scattering, integration of Eq. (22) over t results in

$$\frac{d^2\sigma}{dM_1^2 dM_2^2} = \frac{b_{SD}^2}{b_{el} (2b_{SD} - b_{el})} \frac{\frac{d\sigma}{dM_1^2} \cdot \frac{d\sigma}{dM_2^2}}{\sigma_{el}} \quad (23)$$

Further integration, over M_1^2 and M_2^2 , yields Eq. (6) of Section II, where the coefficient containing the slope parameters was denoted as K_{DD} . Using Eq. (23), a measurement of the ratio of the double to the single diffraction dissociation cross sections may be combined with results for σ_{el} and b_{el} from another experiment to yield the diffractive slope, b_{SD} .

In summary, the method proposed here for measuring diffractive masses is suitable for high mass states, which have high charged multiplicities, and therefore particularly appropriate for the Fermilab Collider. Furthermore, it is unique in its application to double diffraction dissociation, the study of which would normally involve measuring the momenta of all secondary particles, charged and neutral.

IV. APPARATUS

The expected uncertainty in the mean angle $\bar{\theta}$, as calculated from Eqs. (13) and (20), is

$$\frac{\delta\bar{\theta}}{\bar{\theta}} = \pm \frac{0.5}{\left(\frac{\sqrt{s}}{2} \bar{\theta}\right)^{\frac{1}{2}}} \quad (\sqrt{s} \text{ in GeV}) \quad (24)$$

The experimental angular resolution must be comparable to this uncertainty in order not to limit the accuracy of the mass measurement. In addition, the experiment must be capable of measuring high charged multiplicities. At $\sqrt{s} = 2000$ GeV, the charged multiplicity distribution from a hard core collision is expected^[4] to peak at $\bar{n} = 2s^{\frac{1}{4}} = 89$ and have a width $D = \bar{n}/2 = 45$. This corresponds to > 180 particles at two standard deviations above the mean multiplicity, representing 2.3% of the hard core events, or $\sim 1\%$ of the inelastic cross section.

The apparatus shown in Figure 9 has these properties. It consists of scintillation counter hodoscopes surrounding the entire interaction region outside a polar angle of 5 mrad. There are no counters inside the beam pipes. A total of 420 counters are employed, 210 on each side of the interaction region. For simplicity in construction, the counters have the same width and are mounted on "wheels" of the same size, about 1m in diameter. The distance from the interaction region is such that the angular bins defined by the counter size are somewhat smaller than the expected uncertainty in the mean angle given by Eq. (24). The number of bins is sufficient to handle the expected large charged multiplicities.

The counters will be timed for particles assumed to originate in the interaction region and will be triggered with a majority coincidence requiring five or more particles, corresponding to one standard deviation below the mean multiplicity for $M_x = 20$ GeV. Beam-gas events with particles on both sides of the interaction region will be rejected by the timing. Those with particles only on one side, if proved to be a problem, can be eliminated by using additional counters closer to the interaction region. Since the smallest mass we intend to measure is 20 GeV, the smallest $\bar{\theta}$ of interest is 20 mrad, corresponding to a distance of 5cm from the beam at 2.5m from the interaction region. Therefore, counters surrounding the beam pipe can be used in this position to reduce (in coincidence) and to study (in anti-coincidence) beam-gas events. The pulse height, recorded for each counter, may prove useful in rejecting counts due to general room background.

V. EVENT RATES AND RUNNING TIME

At $\sqrt{s} = 2000$ GeV, the total $\bar{p}p$ cross section is expected to lie somewhere between the values of 62 mb and 78 mb, representing respectively the $\ln s$ and the $\ln^2 s$ extrapolation of the ISR data (see Fig. 21 in Ref. 2). For the purpose of calculating the expected rates in this experiment, we take $\sigma_T = 70$ mb. We then have^[1]

$$\sigma_T = \sigma_o + \sigma_{e\ell} + 2 \sigma_{SD} + \sigma_{DD} = 70 \text{ mb}$$

$$\sigma_o = 26.3 \text{ mb}$$

$$\sigma_{e\ell} = 0.175 \sigma_T = 12.3 \text{ mb}$$

$$\sigma_{SD} = 0.68 \ln(0.1s) = 8.8 \text{ mb}$$

$$\sigma_{DD} = \sigma_T - \sigma_o - \sigma_{e\ell} - 2\sigma_{SD} = 14.0 \text{ mb}$$

$$\sigma_{in} = \sigma_T - \sigma_{e\ell} = 57.7 \text{ mb}$$

The differential cross sections for single and double diffraction dissociation are (from Eqs. 5,6 and 23):

$$\frac{d\sigma_{SD}}{dM_x^2} = \frac{0.68 \text{ mb}}{M_x^2} \quad (25)$$

$$\frac{d^2\sigma_{DD}}{dM_1^2 dM_2^2} = \frac{\sigma_{DD}}{\sigma_{SD}^2} \frac{d\sigma_1}{dM_1^2} \frac{d\sigma_2}{dM_2^2} \quad (26)$$

Within the full width of the M^2 resolution, $\Delta M^2 = 2\delta M^2$, which may be expressed in terms of $1-x$ using Eq. (20), we obtain $\Delta\sigma_{SD} = 0.20 (1-x)^{-1/8}$ mb and $\Delta\sigma_{DD} = 0.007 [(1-x_1)(1-x_2)]^{-1/8}$ mb.

Using the above cross sections, the expected event rates may now be calculated. At a luminosity of $10^{28} \text{ cm}^{-2} \text{ sec}^{-1}$, the total number of events triggering the apparatus, corresponding to σ_{in} , will be $\sim 2 \times 10^5$ /hour. Within the full width of the M^2 resolution, the number of single diffraction dissociation events at $1-x = 0.1$ will be $\sim 10^4$ /hour, while the number of double diffraction dissociation events at $1-x_1 = 1-x_2 = 0.1$ will be ~ 400 /hour.

Thus, 500 hours of running will be sufficient for the proposed study even if the luminosity is down by two orders of magnitude, as may be the case in the initial stages of the operation of the Collider.

VI. LOCATION OF EXPERIMENT

This experiment is being proposed for the D0 experimental area. However, since there are no special requirements on beam characteristics, the experiment may be performed in any one of the interaction regions.

REFERENCES

- 1]. K. Goulianos, "Diffractive Interactions of Hadrons at High Energies," Rockefeller University Report No. RU 81/A-23, submitted to The International Conference on High Energy Physics, Paris, France, July 26-31, 1982.
- 2]. A. White, AIP Conf. Proc. No. 85 - Proton-Antiproton Collider Physics-1981 (Madison, Wisconsin), V. Barger, D. Cline, F. Halzen (Eds.), (American Institute of Physics, New York, 1982) pp. 363-434.
- 3]. R.L. Cool et al., Phys. Rev. Lett. 48, 1451 (1982).
- 4]. K. Goulianos et al., Phys. Rev. Lett. 48, 1454 (1982); K. Goulianos, AIP Conf. Proc. No. 85 - Proton-Antiproton Collider Physics-1981 (Madison, Wisconsin), V. Barger, D. Cline, F. Halzen (Eds.), (American Institute of Physics, New York, 1982) pp. 469-485.
- 5]. G. Bellettini, AIP Conf. Proc. No. 15 - High Energy Collisions-1973 (Stony Brook), Chris Quigg (Ed.), (American Institute of Physics, New York, 1973) pp. 9-46.
- 6]. Y. Akimov et al., Phys. Rev. D14, 3148 (1976).

FIGURE CAPTIONS

- Fig. 1 - Proton-proton cross sections as a function of laboratory momentum. After subtraction of twice the single diffraction dissociation cross section, as given by Eq. 5, the remaining rise of the inelastic cross section with energy is small and consistent with the expected contribution from double diffraction dissociation, as explained in the text [from Ref. 1].
- Fig. 2 - Rapidity distribution of charged particles from an isotropic decay of a diffractive state of mass M , for pp collisions at $(\text{c.m. energy})^2 = s$ (see Eqs. 16, 17 and 18 in text).
- Fig. 3 - Rapidity distributions of charged particles from isotropic decays of diffractive states X , for $pp \rightarrow Xp$ at $\sqrt{s} = 2000$ GeV.
- Fig. 4 - Distributions of the mean rapidity $\bar{\eta}$ for events with a given $\Delta\eta$ and fixed charged multiplicity, from pp collisions at $p_{\text{ISR}} = 31.4$ GeV at the ISR [from Ref. 5].
- Fig. 5 - The mean rapidity versus the rapidity width at various charged multiplicities, for events from pp collisions at $p_{\text{ISR}} = 31.4$ GeV at the ISR [from Ref. 5].
- Fig. 6 - The inclusive single diffraction dissociation cross section $d^2\sigma/dtdM_x^2$ versus M_x^2 for $pp \rightarrow Xp$ at $|t| = 0.025$ $(\text{GeV}/c)^2$ and $s = 500$ GeV^2 [from Ref. 6].
- Fig. 7 - The differential cross section $d\sigma/dx$ versus $1-x$ for $pp \rightarrow Xp$ at $\sqrt{s} = 2000$ GeV. The solid and broken curves are explained in the text. The ladder-like steps represent the full width of the resolution expected in this experiment.

Fig. 8 - The inclusive single diffraction dissociation cross section $d\sigma/dM_x^2$ as a function of M_x^2 for $pp \rightarrow Xp$ at $\sqrt{s} = 60$ GeV (ISR), 540 GeV (SPS Collider), and 2000 GeV (Fermilab Collider). The broken curves represent the cross sections that would presumably be obtained in measurements using the recoil technique. Our method is expected to yield the solid curve, representing $1/M_x^2$ behavior. The cut-off at $M_x^2/s \cong 0.35$ is due to t_{\min} (see text). The ladder-like steps represent the full width of the resolution obtainable by our method.

Fig. 9 - Apparatus. The interaction region is surrounded by scintillation counters represented by the small boxes in the side view and by the $6 \times 9 = 54$ sections in the front view. There are no counters in the beam pipes.

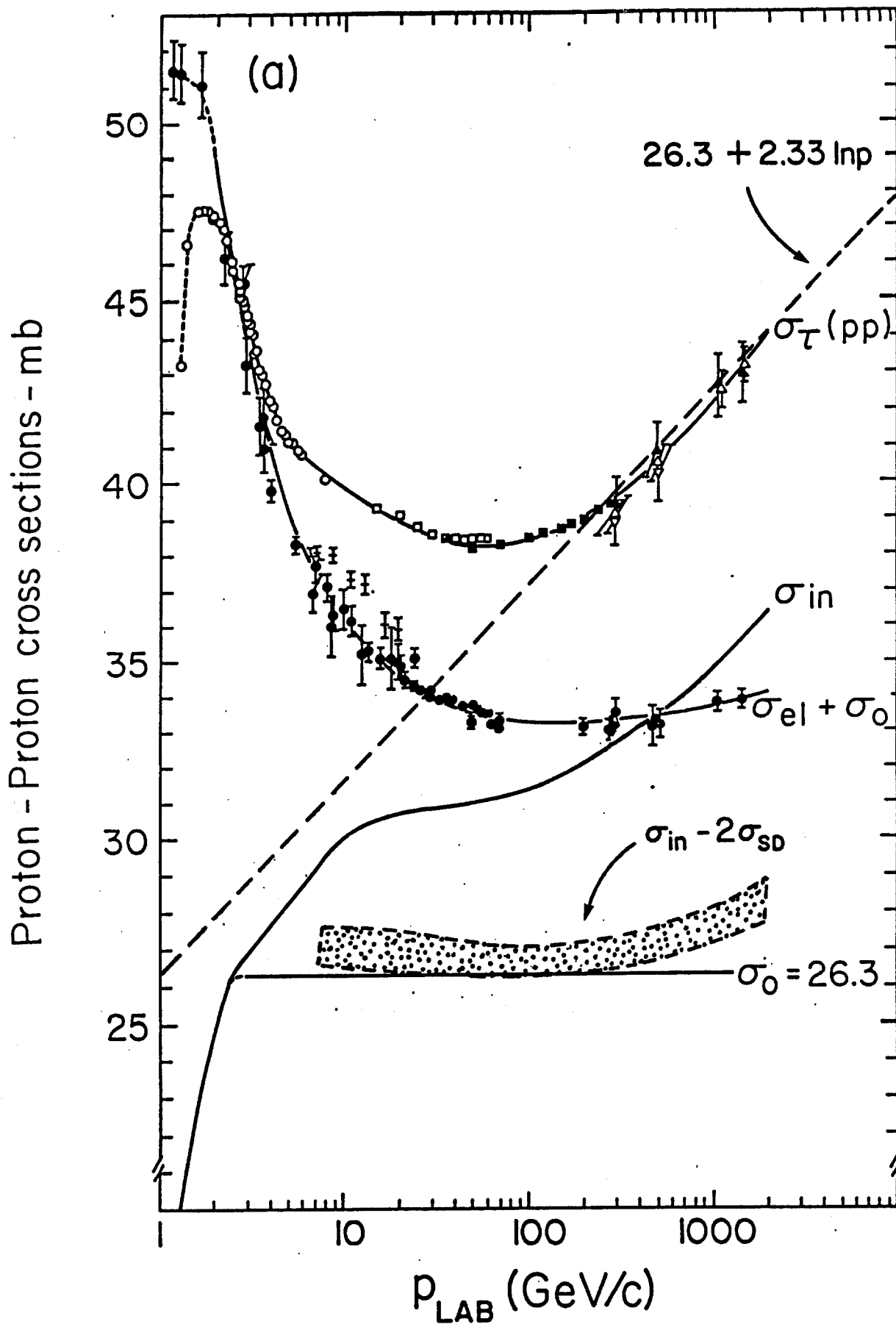


FIG. 1

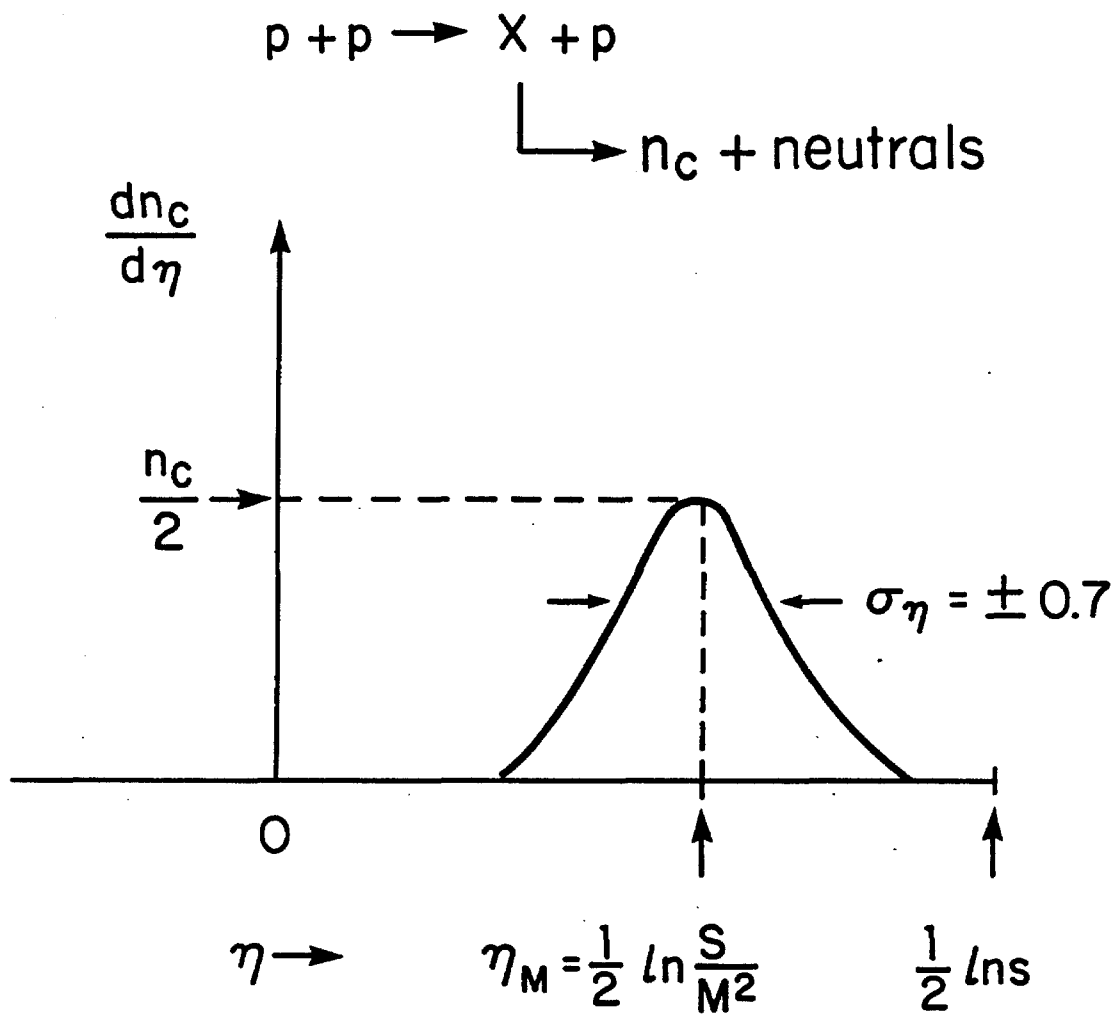


FIG. 2

$p + p \rightarrow X + p$ at $\sqrt{s} = 2000$ GeV

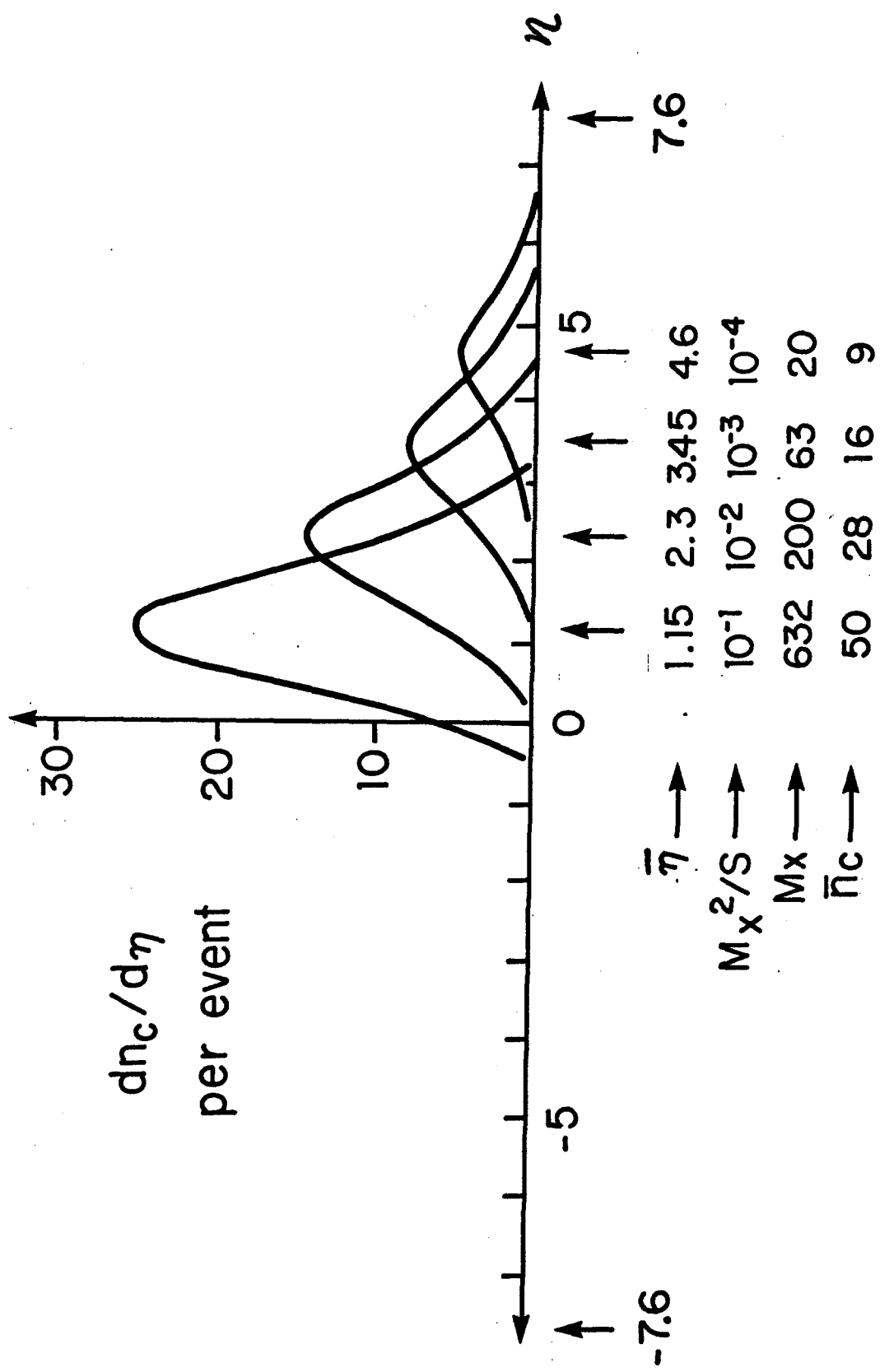


FIG. 3

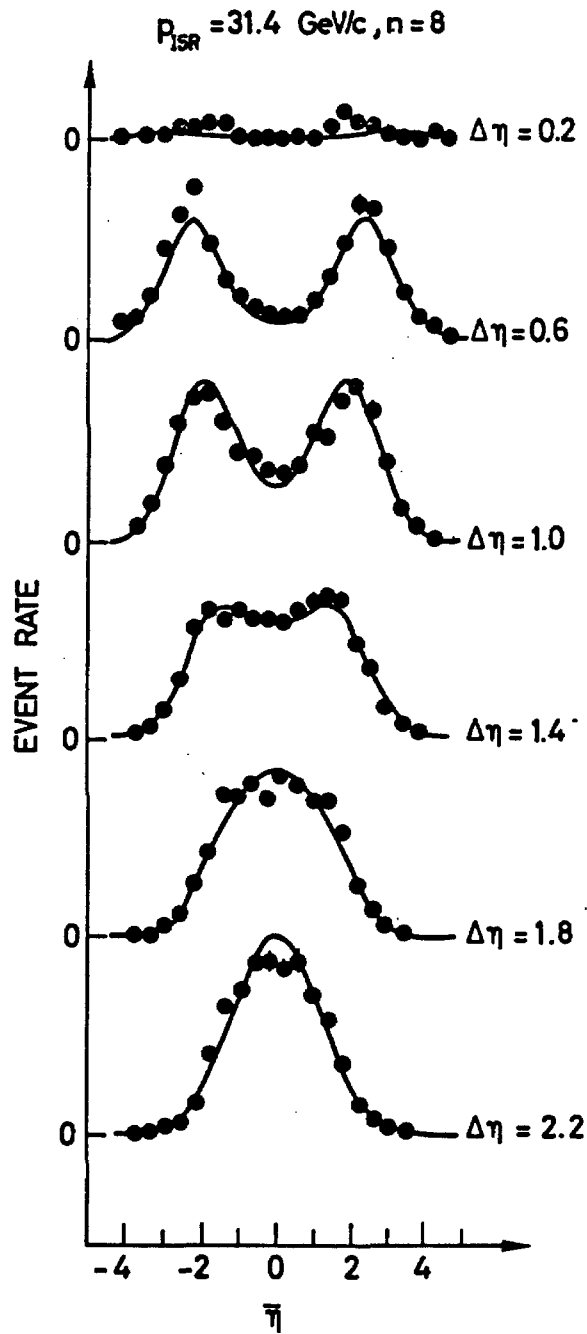


Fig. 12 Distribution of events of multiplicity 8 at $p_{ISR} = 31.4 \text{ GeV}/c$ versus $\langle \eta \rangle = \sum \eta_i / (n - 2)$ (leftmost and rightmost tracks removed), for various values of the dispersion $\Delta \eta = \sqrt{\sum (\eta_i - \langle \eta \rangle)^2 / (n - 3)}$.

PISA STONY BROOK
CLUSTERING OF EVENTS IN THE η , $\Delta\eta$ PLANE
 $p_{ISR} = 31.4 \text{ GeV/c}$

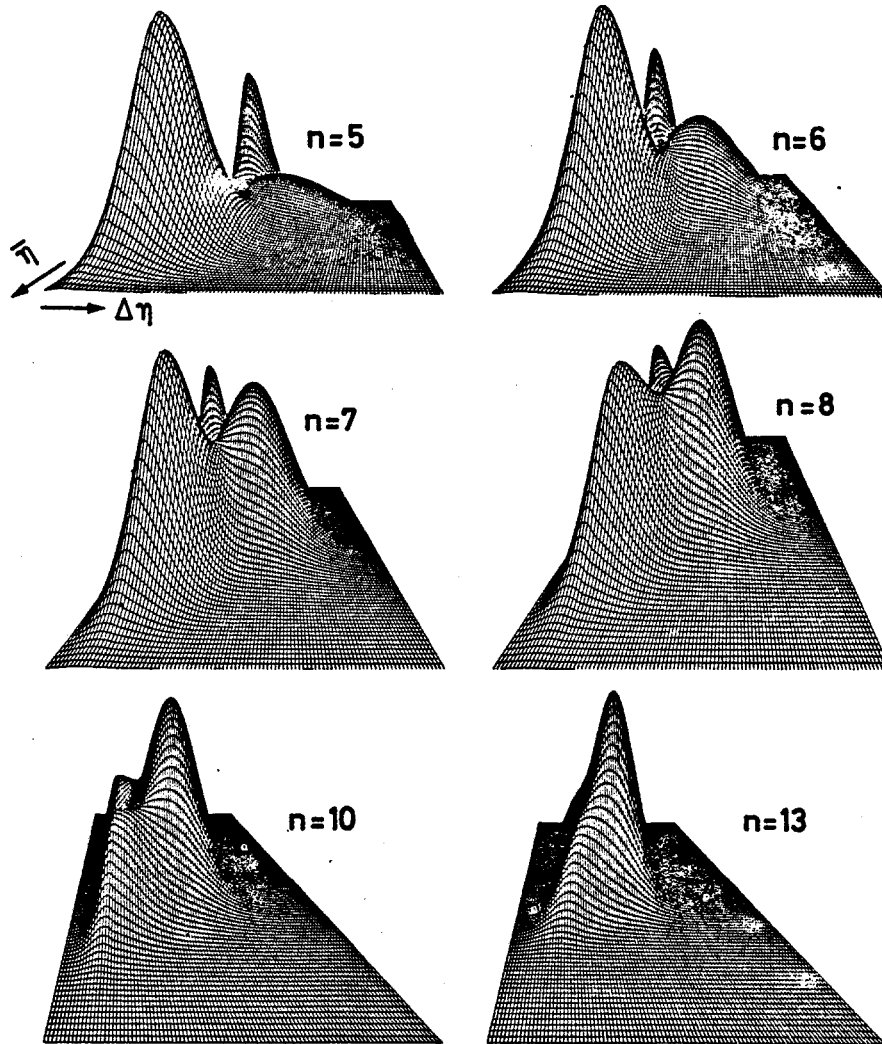


Fig. 16 Three-dimensional view of event distribution in the $\langle\eta\rangle$, $\Delta\eta$ plane, for various multiplicities at $p_{ISR} = 31.4 \text{ GeV/c}$.

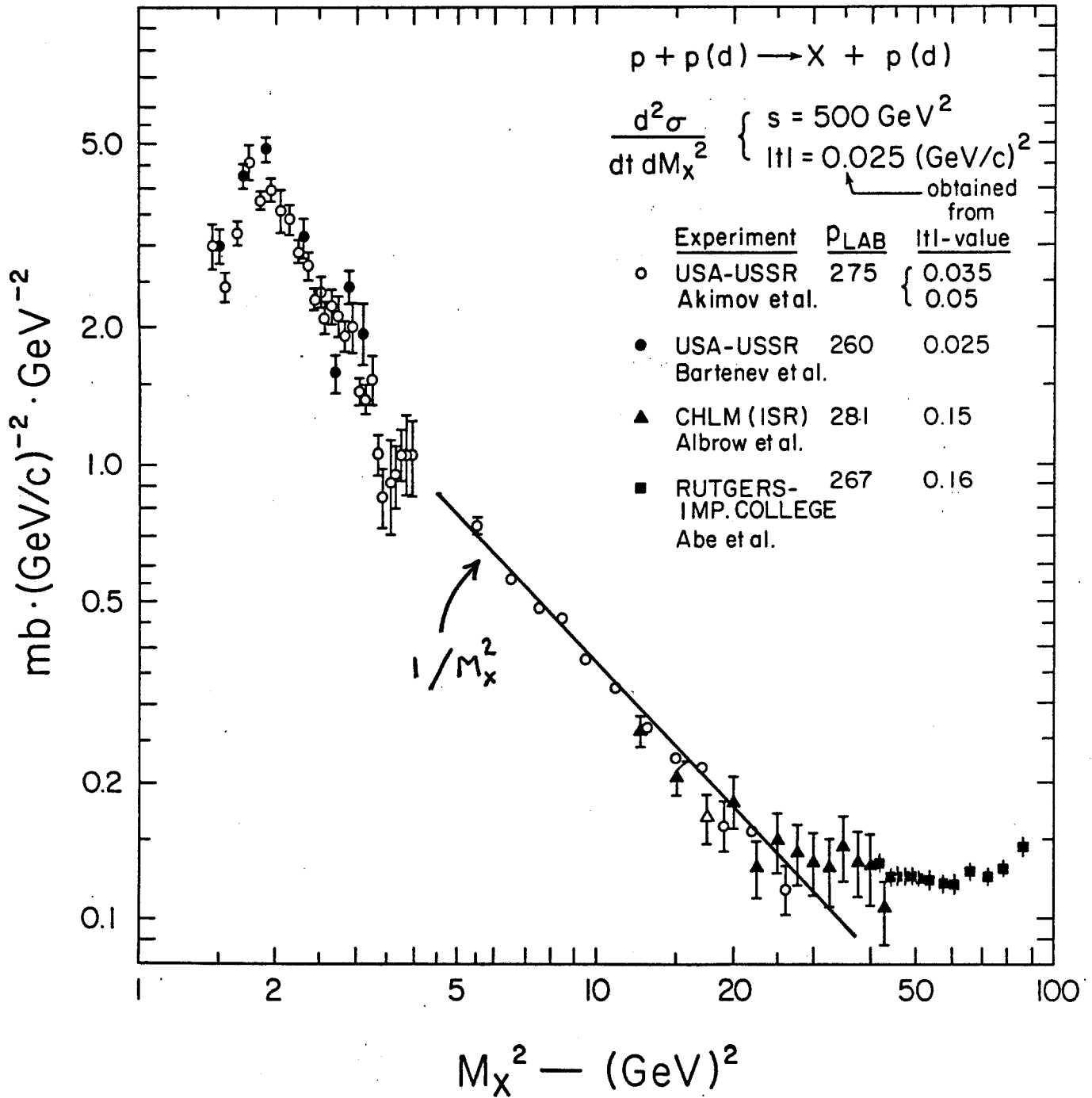


FIG. 6

$pp \rightarrow Xp$ at $\sqrt{s} = 2000$ GeV

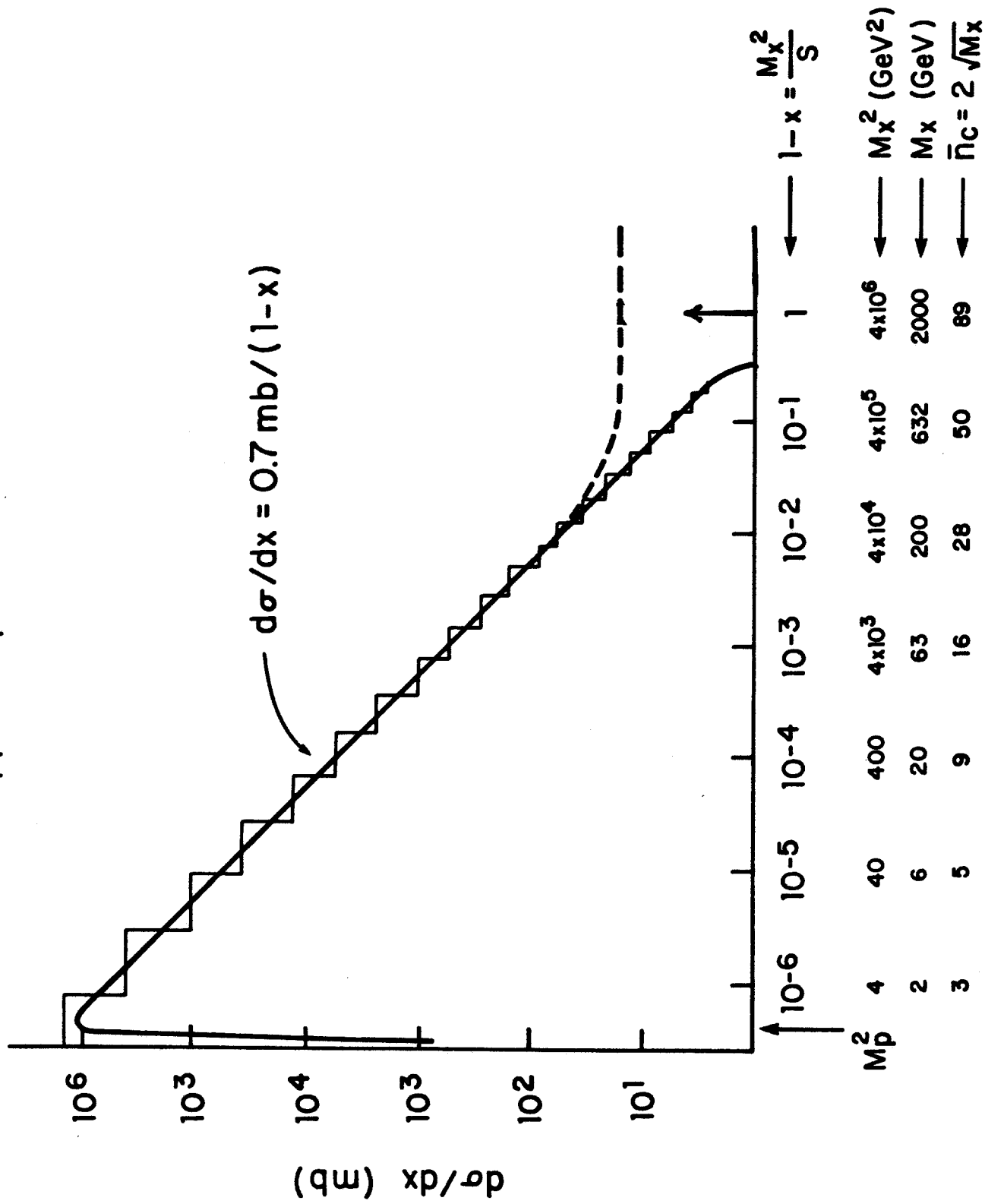


FIG. 7

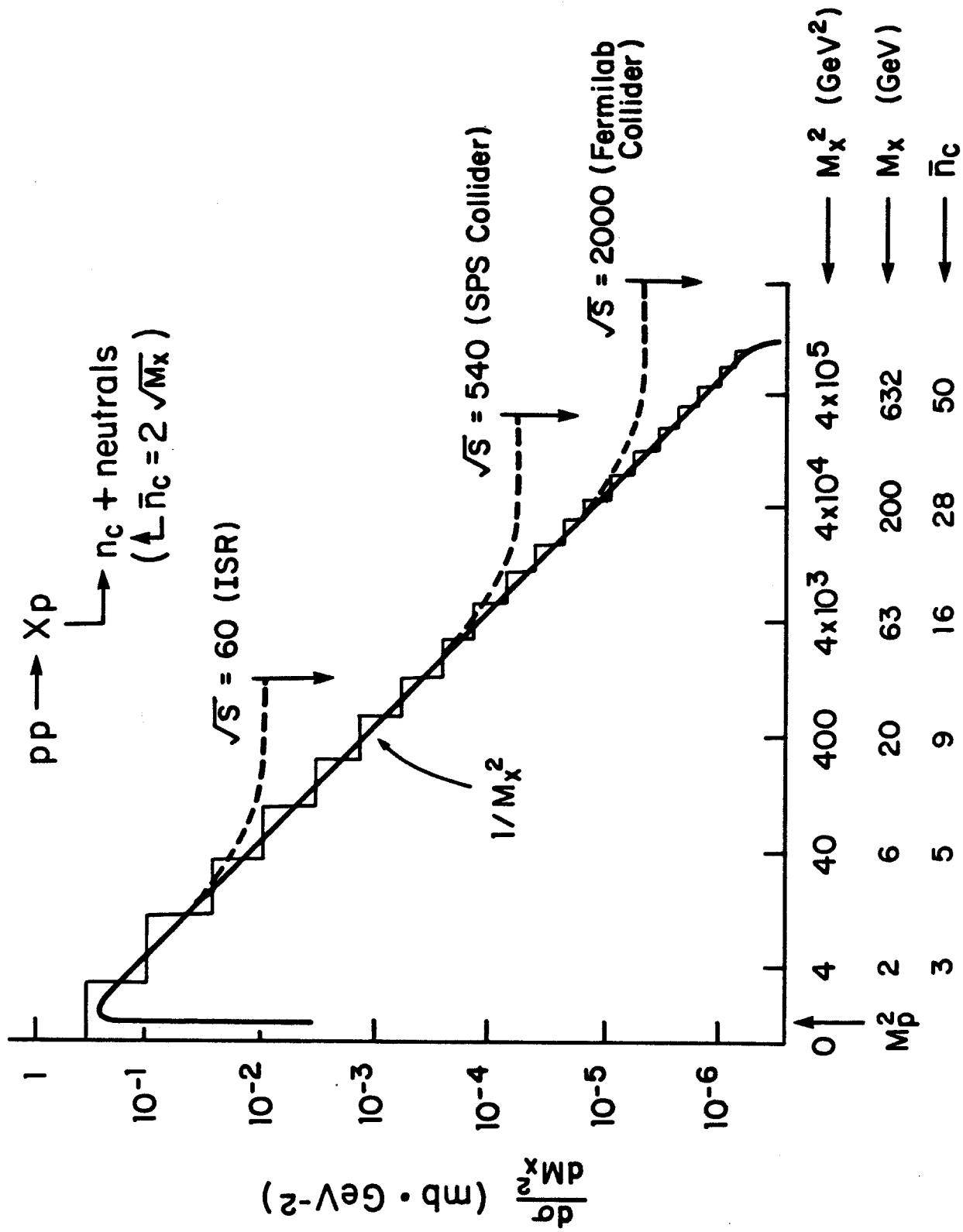
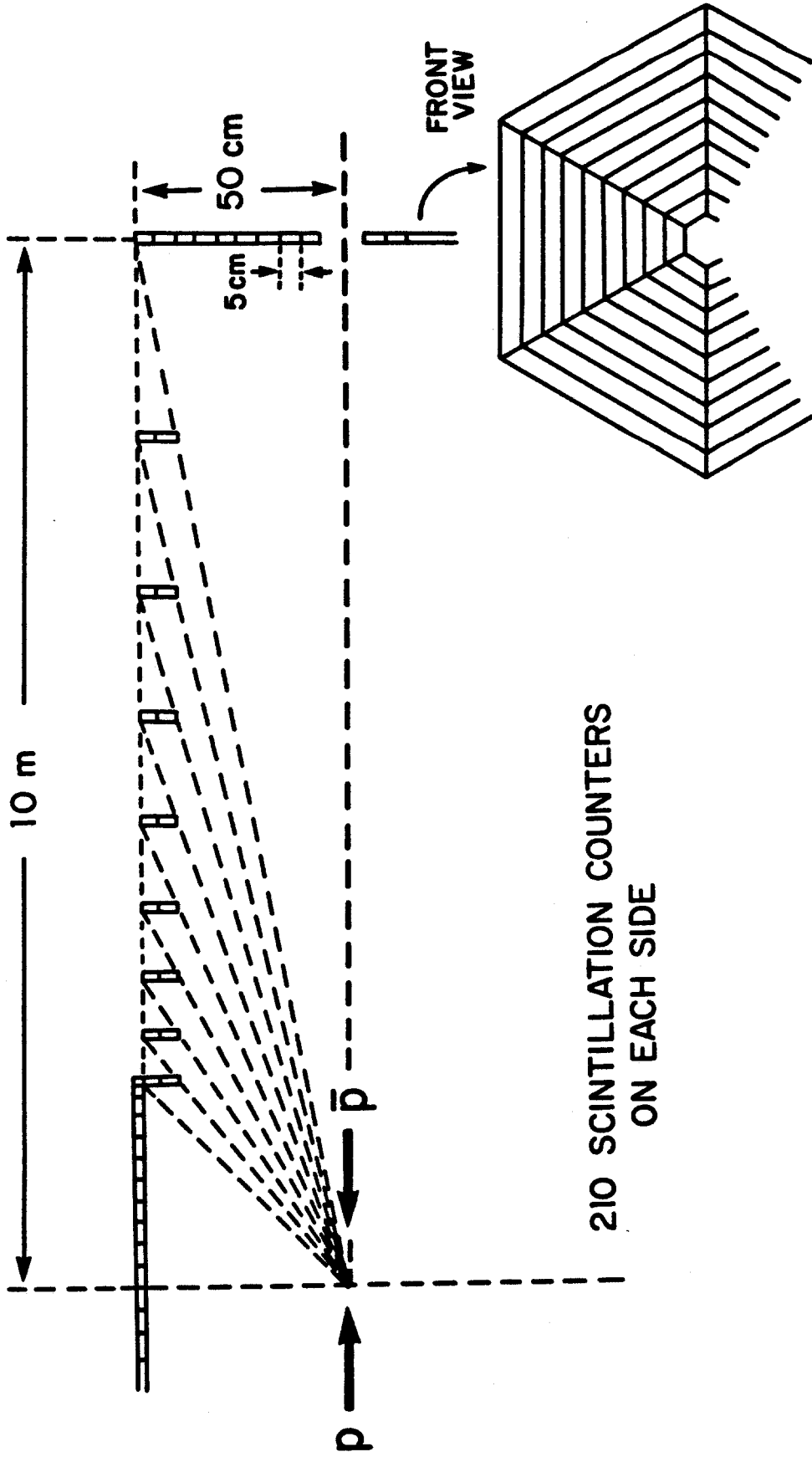


FIG. 8



210 SCINTILLATION COUNTERS
ON EACH SIDE

FIG. 9